Radiocarbon, Vol 61, Nr 5, 2019, p 1441–1448 DOI:10.1017/RDC.2019.73
Selected Papers from the 23rd International Radiocarbon Conference, Trondheim, Norway, 17–22 June, 2018
© 2019 by the Arizona Board of Regents on behalf of the University of Arizona

A NOVEL DEDICATED HVE ^{14}C AMS SYSTEM

M Klein* • N C Podaru • D J W Mous

High Voltage Engineering Europa B.V., Amersfoort, The Netherlands

ABSTRACT. High Voltage Engineering Europa (HVE) has designed a vacuum-insulated tandem accelerator dedicated to radiocarbon (^{14}C) analysis. A unique feature of the design is a magnetic charge state selector that is incorporated in the high voltage terminal, which reduces the primary source of background that originates from the injection of $^{13}CH^-$ to negligible levels. As a result, background levels in the low 10^{-16} regimes are anticipated, thus supporting the most stringent ^{14}C dating applications. Another feature of the system is the incorporation of several slit feedback loops for stabilization of the position of the ion beam throughout the system, which avoids drift and ensures stable, long-term operation. Finally, this article presents measurements and quantitative analysis of background contributions from $^{13}CH^-$.

KEYWORDS: ^{14}C dating, radiocarbon, vacuum insulated accelerator.

INTRODUCTION

Accelerator mass spectrometers with >1 MV tandem particle accelerators are operating around the world since the 1980s. Amongst the most commonly used rare isotopes, we mention ^{10}Be ^{14}C, ^{26}Al, ^{41}Ca, ^{129}I, ^{236}U, and $^{239/240}$Pu. By far, the most common isotope used for dating is ^{14}C. Furthermore, ^{14}C is extensively used in biomedical tracing studies. Early high-performance AMS systems were able to achieve ^{14}C background levels in the order of 10^{-16} by using two magnets in the high-energy spectrometer and charge state 3+. Almost a decade ago, experiments conducted at ETH Zurich demonstrated that ^{14}C AMS could be performed in tandem accelerators with terminal voltages as low as 200 kV by using the charge state 1+ (Synal et al. 2007). The system uses only one analyzing magnet in the high energy side of the spectrometer and has a typical background level of 10^{-15}.

Although for sub-MV AMS systems a substantial number of publications and theses (Schulze-König et al. 2011; Seiler 2014; Maxeiner at al. 2015), dealt with the details and origins of background reduction, a complete and thorough quantitative understanding of these contributions is still lacking. Consequently, sub-MV systems have not yet achieved background levels in the low 10^{-16}.

At HVE we have experimentally investigated the sources of background in a ~200 kV accelerator system and developed a novel vacuum-insulated accelerator system aiming to deliver background levels in the low 10^{-16} range.

The Model 4102Bo-AMS Radiocarbon Dating System

The newly designed 210 kV AMS system is shown in Figure 1 and has a footprint of 3 m × 2.8 m. The carbon ion beam is produced in the hybrid (solid or gas target) SO110-C sputter ion source (Klein at al. 2017). The normalized emittance of the ion source is 2 – 4 mm mrad $\sqrt{}$MeV up to 250 eμA $^{12}C^-$ (Klein et al. 2013). An XYZ motor driven stage and computer automation are used to auto-tune the ion beam extraction system after source head servicing. The ion beam extraction energy is 40 keV. The low-energy mass spectrometer consists of a 90° H-type dipole magnet with permanent magnets. The magnet gap supports a source divergence as large as 35 mrad for flat-topped transmission. To enable sequential injection of the 3 isotopes by the

*Corresponding author. Email: info@highvolteng.com.

https://doi.org/10.1017/RDC.2019.73 Published online by Cambridge University Press

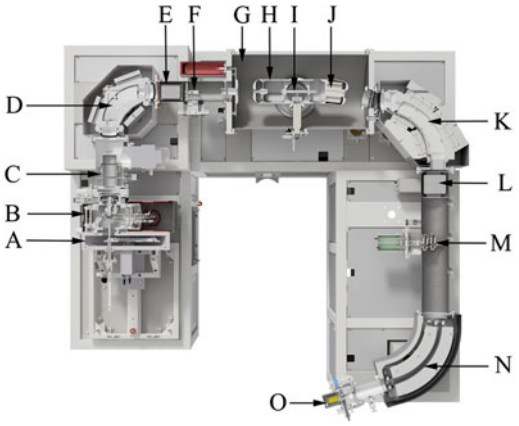


Figure 1 Layout of the 4102Bo-AMS system, showing: A) sample chamber with sample carousel; B) ion source chamber; C) einzel lens; D) bouncer magnet with high voltage enclosure; E) Y-steerer with ion beam blanking capability; F) ^{12}C offset Faraday cup; G) accelerator vessel; H) high-voltage terminal; I) stripper canal; J) magnetic charge state selector; K) high-energy analyzing magnet; L) Y-steerer; M) ^{12}C and ^{13}C offset Faraday cups; N) electrostatic analyzer; and O) ^{14}C gas ionization detector.

bouncing technique, the entire H-type magnet, including yoke, is electrically isolated in a high-voltage enclosure. ^{12}C, ^{13}C, and ^{14}C are bounced at a frequency of 100 Hz for sequential transport through the tandem accelerator. The injection periods are 100 μs for the stable isotopes, and the ^{14}C counting efficiency is >90%.

The tandem accelerator operates at a nominal terminal voltage of somewhat over 200 kV. It is vacuum insulated, and its in-house developed high-voltage power supply is incorporated in the accelerator vessel. In the stripper canal, helium gas is used for ion beam stripping, resulting in low emittance increase due to small-angle scattering.

Pumping is applied for both sides of the stripper canal by a 600 L/s turbo-molecular pump located at ground potential. It reduces the gas flow towards the low and high-energy acceleration gaps, which in turns reduces unwanted charge-exchange processes that would otherwise lead to increased background levels. The diameters of the stripper canal and the pump restrictions follow the beam envelope as calculated with first order matrix formalism. The exit was further enlarged to accommodate the additional beam phase-space increase caused by scattering in the stripper gas. To minimize the required gas flow, the diameter is the smallest at the beam waist in the center of the stripper canal. A second 600 L/s turbo-molecular pump at the accelerator vessel itself ensures adequate vacuum levels in the acceleration gaps.

A novel feature of the accelerator is a charge state selector located in the accelerator terminal, after the stripper canal. It comprises an all-permanent-magnet based H-type magnet mounted around the stripper exit pump restriction (see J in Figure 1). It has a bending angle of 12°, sufficient to resolve charge state 1+ from charge state 2+.

https://doi.org/10.1017/RDC.2019.73 Published online by Cambridge University Press

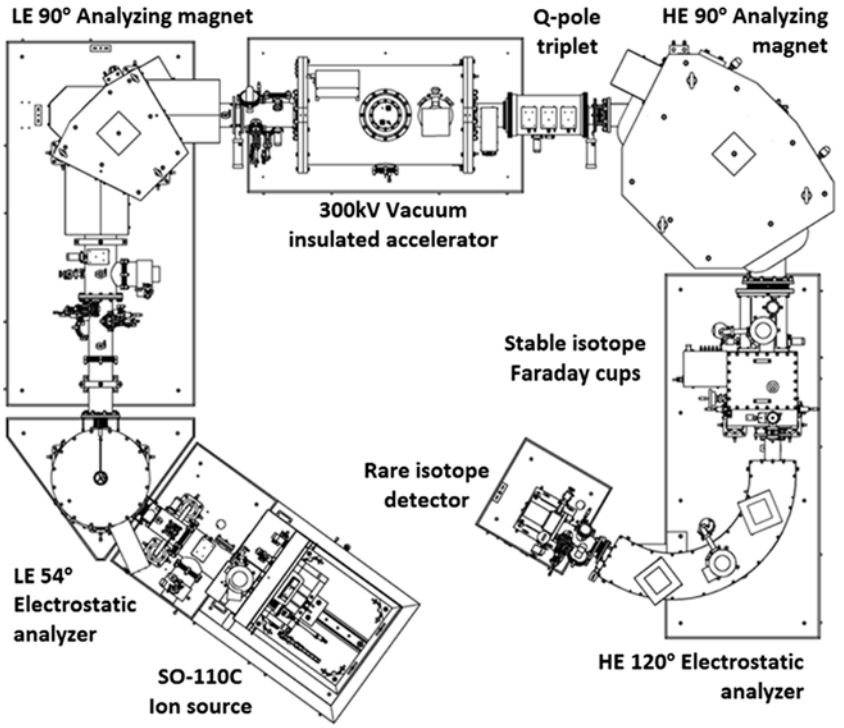


Figure 2 The layout of the 300 kV vacuum-insulated multi-isotope system.

The high-energy spectrometer includes an all-permanent-magnet 78° analyzing magnet with 400-mm bending radius and a spherical ESA, forming an achromatic ion-optical system. The stable isotopes are measured in offset Faraday cups after the analyzing magnet, while ^{14}C is counted in a single-anode gas ionization detector. One Y-steerer is used to correct small misalignments.

An additional feature of the ^{14}C AMS system is the slit stabilization for the ion beam. It is realized by pairs of electrodes inside the Faraday cups that are mounted with a vertical or horizontal slit between them. Comparing the beam current measured on these electrodes provides information on the beam position. Such slit systems are present in the low-energy ^{12}C offset Faraday cup (for X & Y correction using extraction voltage and LE Y steerer, respectively), in the high-energy ^{13}C Faraday cup (for X correction, using the terminal voltage) and the high-energy ^{12}C Faraday cup (for Y correction, using the HE Y steerer). They ensure stable beam position in the stripper canal and in the ^{14}C detector, respectively. As such, position drifts are avoided, and long-term and stable operation is ensured.

^{14}C Background Limits—an Experimental Investigation

To understand the contributions to the background in the ^{14}C AMS system, we used the compact-version HVE AMS system as described in previous works (Klein at al. 2006) and depicted in Figure 2. The 1 MV Tandetron was substituted by a 300 kV vacuum-insulated tandem accelerator operating at 200 kV terminal voltage. Measurements and considerations indicated that the following contributions play no significant role at 10^{-16} background levels:

https://doi.org/10.1017/RDC.2019.73 Published online by Cambridge University Press

- $^{14}NH^-$ with 14/15th injection energy of the reference energy.
- The molecular breakup of $^{13}CH^-$ by residual gas interaction after the LE analyzing magnet and before acceleration.
- Charge exchange processes in the low-energy analyzing magnet or low-energy acceleration gap.
- Contributions from ^{12}C originating from $^{12}CH_2^-$. These are rather similar to background contributions originating from $^{13}CH^-$, albeit being at a lower level.
- Memory effects in the ion source (Arnold et al. 2010).

The measured background level is approximately 10^{-14}. Our experiments identified that the dominant sources of background are related to the injection of molecular $^{13}CH^-$ along with $^{14}C^-$. Because the natural abundance of ^{13}C is ~10^{-2} and the molecular contribution by CH^- is also ~10^{-2} (depending to some extent on sample preparation), the injection of $^{13}CH^-$ is typically at the 10^{-4} level compared to $^{12}C^-$. In the terminal stripper, $^{13}CH^-$ is dissociated and stripped to $^{13}C^{1+}$ with a charge-exchange efficiency of ~45% and to $^{13}C^{2+}$ with a charge-exchange efficiency of ~20%.

Three background contributions from $^{13}C^{1+}$ were identified referred to as I, II, and III. We assume that the ^{13}CH dissociation in the stripper is complete enough to exclude background contribution.

- Type I: $^{13}C^{1+}$ having the same magnetic rigidity ME/q^2 as the $^{14}C_{ref}$ ion
- Type II: $^{13}C^{1+}$ having the same electrostatic rigidity E/q as the $^{14}C_{ref}$ ion
- Type III: $^{13}C^{1+}$ originating from the primary stripping process

Types I and II relate to the interaction of the ^{13}C beam with the residual gas present in the high-energy acceleration gap. After charge exchange to 2+, a small fraction of these $^{13}C^{2+}$ will charge-exchange back to $^{13}C^{1+}$, leaving the accelerator with slightly higher energy. Depending on the position of this second charge-exchange process, the additional energy can give the $^{13}C^{1+}$ the same magnetic mass-energy product (ME/q^2), or the same electrostatic rigidity (E/q) compared to the reference $^{14}C^{1+}$.

Type III background originates from the primary stripping process in the stripping canal in the high-voltage terminal. It has lower energy than the $^{14}C_{ref}$ ion, and a lower magnetic, as well as electrostatic rigidity, compared to the $^{14}C_{ref}$ ion. It will be suppressed in the high-energy magnet as well as in the high-energy ESA. Figure 3 shows the ambiguity bands for magnetic filters in ME/q^2 and electric filters for E/q. Also the type III background is indicated.

In Table 1, the charge-exchange probability in the high-energy accelerating gap is indicated to be 3×10^{-5}. It is calculated by assuming a charge-exchange cross-section $\sigma_{+2,+1}$ for 200 keV carbon in helium of 3×10^{-16} cm^2 (2), a helium pressure in the high-energy accelerating gap of 2×10^{-5} mbar and an interaction length of 2 mm. Measured suppression factors (probabilities) in the high-energy magnet and the high-energy electrostatic analyzer are discussed in the following paragraphs.

https://doi.org/10.1017/RDC.2019.73 Published online by Cambridge University Press

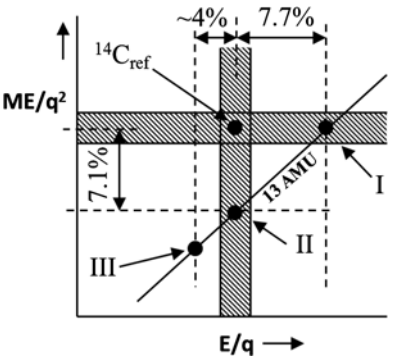


Figure 3 Types I, II, and III backgrounds with their magnetic and electrostatic rigidities.

Background from Magnetic Ambiguity (Contributions I and III)

In case $^{13}C^{1+}$ has an identical magnetic rigidity as the reference $^{14}C^{1+}$, the suppression in the high-energy spectrometer is determined by the electrostatic analyzer (ESA). The difference in electrostatic rigidity is calculated to be +7.7% and –3.9% for type I and type III backgrounds, respectively. To determine the suppression by the ESA, a low-intensity $^{12}C^{1+}$ is directed into the entrance of the ESA. The ESA voltage was scanned, and the detector counts were recorded, see Figure 4. The central peak of the scan at 16.26 kV (point A) represents the "$^{14}C_{ref}$" contribution (normalized to 1). The contributions I and III are found by dividing the reference ESA voltage setting by 1.077 (= 15.10 kV), and 0.961 (= 16.92 kV), respectively. Note that at both sides of the central peak "A," the local minima indicated by "B" correspond to the beam located in between the entrance of the detector and the end of the ESA electrodes. Summarized in the "HE ESA" column of Table 1 are the suppression factors for the ESA for the backgrounds I and III.

Background from Ambiguity in Electrostatic Rigidity (Contributions II and III)

In case $^{13}C^{1+}$ has an identical electrostatic rigidity as the reference $^{14}C^{1+}$, the high-energy magnet determines the suppression in the high-energy spectrometer. The difference in magnetic rigidity is calculated to be –7.1% and –10.7% for type II and type III backgrounds, respectively.

The suppression by the high-energy analyzing magnet was measured by scanning by the magnet during a low-intensity $^{12}C^{1+}$ beam at a constant ESA setting that corresponds to the reference $^{14}C^{1+}$ energy. Figure 5 depicts the results.

The central peak corresponds to the ^{14}C reference path while contributions II and III are at $106.45A/\sqrt{0.929} = 110.5$ A and $106.45A/\sqrt{0.893} = 112.7$ A, respectively. Summarized in Table 1 under column "HE magnet" are the suppression factors of contribution II and III by the high-energy analyzing magnet.

DISCUSSION

It should be noted that the measurements cover a broad dynamic range, of ~7 orders of magnitude. In practice, the scans that are shown in Figures 4 and 5 consists of several

https://doi.org/10.1017/RDC.2019.73 Published online by Cambridge University Press

https://doi.org/10.1017/RDC.2019.73 Published online by Cambridge University Press

Table 1 This table summarizes the three major contributions to the background of the system, resulting from $^{13}CH^-$ injection. Data shown are relative to $^{14}C_{ref}$. The background is calculated from the various contributions to the total suppression ("Total"), assuming $^{13}CH/^{12}C = 10^{-4}$ and assuming a $^{14}C^+$ yield of 45% in the stripping process: Background = Total $\times 10^{-4}$ / 45%.

				Probability					
Type	Origin	ME/q^2	E/q	Ch.exch. in stripper	Ch. exch. in HE Accel gap	HE Magnet	HE ESA	Total	Background
I	$^{13}CH^-$ injection & Ch. exch. 2+ -> 1+ in HE Accel gap	1	1,077	0,20	3,0E-05	1	8,0E-06	4,8E-11	1,1E-14
II	$^{13}CH^-$ injection & Ch. exch. 2+ -> 1+ in HE Accel gap	0,929	1	0,20	3,0E-05	1,0E-06	1	6,0E-12	1,3E-15
III	$^{13}CH^-$ injection	0,893	0,961	1	1	4,0E-07	2,0E-06	8,0E-13	1,8E-16

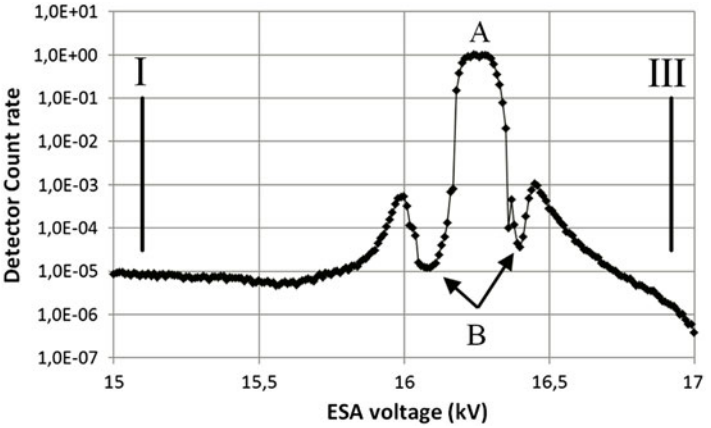


Figure 4 ESA suppression for constant ME/q^2 ion beams. Suppression levels of background types I and III are indicated.

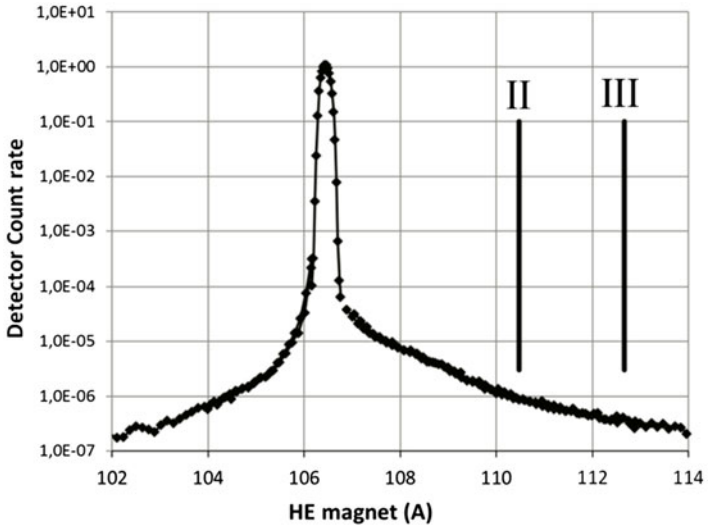


Figure 5 High-energy analyzing magnet suppression for constant E/q ion beams. Suppression levels of background type II and III are indicated.

"sub-scans" with different intensities of the injected $^{12}C^{1+}$. Because of this procedure and the nature of such scans the accuracy of the measured suppressions factors is low, maybe off by a factor 2–3.

Contributions type I and II are related to ions having charge state 2+ after the stripper that change to 1+ within the high-energy acceleration gap. The magnetic charge state selector deflects the potentially interfering 2+ ions before the high energy acceleration. Those ions are stopped before entering the HE magnet or ESA where they could form an ambiguity. This will suppress the background contributions type I and II by at least several orders of

https://doi.org/10.1017/RDC.2019.73 Published online by Cambridge University Press

magnitude, resulting in background contributions in the low 10^{-16} regime for this class of background, or even below.

The type III background does not benefit from the magnetic charge state selector in the high-voltage terminal, but it is anticipated to have the lowest background level. To ensure that this class of background does not contribute to the overall background level, the ESA in the newly designed dedicated ^{14}C system has a gap that is sufficiently large to avoid scattering on the inner electrode.

CONCLUSIONS

In this work, we identified and quantified contributions to the background for sub-MV ^{14}C AMS systems. The two dominant contributions are related to $^{13}CH^-$ injected in the stripper yielding $^{13}C^{2+} \rightarrow {}^{13}C^{1+}$ ions and can be suppressed by incorporating a charge state selector after ion beam stripping. We anticipate that this novel vacuum-isolated accelerator system will have background levels in the low 10^{-16} range, supporting most stringent ^{14}C AMS dating applications. The layout and new feature for high measurement stability of the novel ^{14}C AMS system have been discussed.

REFERENCES

Arnold M, Merchel S, Bourlès DL, Braucher R, Benedetti L, Finkel RC, Aumaître G, Gottdang A, Klein M. 2010. The French accelerator mass spectrometry facility ASTER: improved performance and developments. Nuclear Instruments and Methods in Physics Research B 268(11–12):1954–1959.

Klein M, Mous DJW, Gottdang A. 2006. A compact 1 MV multi-element AMS system. Nuclear Instruments and Methods in Physics Research B 249:764–767.

Klein M, Gottdang A, Mous D. 2013. High-current ^{14}C measurements on an HVE 1MV AMS system. Radiocarbon 55(2):224–230.

Klein M, Mous DJW. 2017. Technical improvements and performance of the HVE AMS sputter ion source SO-110. Nuclear Instruments and Methods in Physics Research B 406:210–213.

Maxeiner S, Seiler M, Suter M, Synal HA. 2015. Charge state distributions and charge exchange cross sections of carbon in helium at 30–258 keV. Nuclear Instruments and Methods in Physics Research B 361:541–547.

Schulze-König T, Seiler M, Suter M, Wacker L, Synal HA. 2011. The dissociation of ^{13}CH and $^{12}CH_2$ molecules in He and N_2 at beam energies of 80–250 keV and possible implications for radiocarbon mass spectrometry. Nuclear Instruments and Methods in Physics Research B 269: 34–39.

Seiler M. 2014. Accelerator mass spectrometry for radiocarbon at very low energies [PhD thesis]. ETH Zurich.

Synal HA, Stocker M, Suter M. 2007. MICADAS: a new compact radiocarbon AMS system. Nuclear Instruments and Methods in Physics Research B 259:7–13.

https://doi.org/10.1017/RDC.2019.73 Published online by Cambridge University Press